Danish Meteorological Institute
Ministry of Transport and Energy

Scientific Report

Microphysical measurements important for microwave remote sensing of sea ice

Field guide

Rasmus Tonboe, Susanne Hanson[2]
[1]Danish Meteorological Institute, [2]Danish National Space Center

July 2006

Photo 1. Ice thickness measurement, North of Alert, Arctic Ocean.

Danish Meteorological Institute
Ministry of Transport and Energy

Colophon

Serial title:
Scientific Report 06-03 06-03

Title:
Microphysical measurements important for microwave remote sensing of sea ice

Subtitle:
Field guide

Author(s):
Rasmus Tonboe, Susanne Hanson

Other contributors:
Sebastian Gerland (Norwegian Polar Institute)

Responsible institution:
DMI

Language:
English

Keywords:
microphysical snow and sea ice measurements, microwave remote sensing

Url:
www.dmi.dk/dmi/sr06-03

Digital ISBN:
87-7478-536-2

ISSN:
1399-1949 (online)

Version:

Website:
www.dmi.dk

Content:

Abstract

Description of the snow and ice parameters relevant for microwave remote sensing and their measurement.

Resumé

Beskrivelse af sne og isparametre med relevans for mikrobølge telemåling og målingen af disse.

Introduction

This report will be used as guidance for the crew onboard the TARA–expedition (2006-2008?) to do snow and ice measurements in the DAMOCLES- project. Tara will be anchored to the perennial ice in The East Siberian Sea September 2006 and drift across the North Pole to the Fram Strait with the transpolar ice drift. The journey is inspired by Nansens Fram (1893-1896) and the Russian drift stations (since 1937). A significant measurement programme including: meteorology, oceanography and snow and ice will result in unique time-series from this expedition. The authors would like to thank Sebastian Gerland from the Norwegian Polar Institute for useful comments.

Why measure? The snow/ice thickness of sea ice and the open water fraction are important parameters, which determine the fluxes between the atmosphere and the Arctic Ocean and are also climate change indicators. Further, snow and ice surface parameters are important for satellite sea ice microwave measurements. State-of-the-art sea ice satellite mapping does not include snow/ice thickness/density. It is therefore difficult even with freeboard measurements from altimeters to estimate ice thickness without large error-bars and climate simulations must as a result accept sparsely sampled sea ice climatology. Snow and ice *in situ* measurements are therefore not only important for sea ice freeboard/thickness mapping in remote regions; they also serve as important data when developing our knowledge of the relationships between satellite data and snow/ice parameters for a sustainable monitoring of the Arctic Ocean. The *in situ* measurements should be combined with ground based or high-resolution airborne microwave measurements.

Parameters important when analysing ground based or high-resolution snow covered sea ice microwave data

The description of the snow profile should include for each distinct layer or selected intervals:
1) thermometric temperature,
2) surface roughness and hardness,
3) density,
4) layer thickness,
5) grain or inclusion size,
6) salinity,
7) liquid water content,
8) classification of the snow or ice type (international glaciology codes),
9) photograph and general description.

Sequences of optically distinct ***layer thickness*** form basis for the profile measurements. Layer homogeneity is generally assumed. The ***thermometric temperature*** is a key parameter for the saline ice permittivity. In particular, the snow surface and snow/ice interface temperatures are important measurements. The

small-scale ***surface roughness*** is a key parameter for radar backscattering and the snow ***density*** is important for the snow and multiyear ice permittivity and consequently both reflection and transmission coefficients. Microwave volume scattering is a function of ***grain or inclusion size*** and its distribution. The ice or saline snow permittivity and in particular the loss is a function of ***salinity*** (and temperature, i.e. brine content). The ***liquid water content*** of the snow is very important for its permittivity and the transition from dry to wet snow is particularly important. The ***general description*** of the profile includes ***classification*** of snow and ice types. The parameters and their measurement are described in this report.

These microphysical parameters are important not only for the microwave scattering and radiation, but also the snow and ice thermodynamic (specific heat and thermal conductivity) and radiation (albedo and extinction) properties, i.e. the energy balance. The parameters and their measurement are described in this report.

Arctic sea ice and snow

In the ocean mixed layer the seawater density (salinity > 24.7 psu) increase as a function of decreasing temperature. New-ice formation begins in the sub-cooled mixed layer (about -1.8˚C). The ice formation produces brine (increase salinity) and together with atmospheric cooling, the mixed layer is unstable and overturned by convection. The initial crystals are stirred in the upper meters by wind-induced turbulence. This stage is called frazil ice. If formation continues under turbulent conditions the frazil ice cover develop into grease ice or pancake ice. Grease ice is the suspension of frazil ice crystals in a flexible and soupy layer. The individual frazil plates may coagulate into clumps, but grease ice is otherwise unconsolidated (Martin & Kauffman, 1981). The rate of frazil and grease ice formation is related to the air temperature and turbulence level of the ocean surface. No direct measurements of grease ice roughness were found in the literature, but an indicator of its smooth surface is the very low radar backscatter, σ_0 , at moderate incidence angles (15˚-60˚). Onstott *et al.* (1998) find in C-band (incidence angle 35˚) the σ_0 of grease ice to be about -27 dB. The volumetric ice crystal concentration in the grease ice layer is larger than about 15 % and less than about 40 % before it starts consolidating (Martin & Kauffman, 1981; Weeks & Ackley, 1986). The salinity of the grease ice layer is reduced compared to seawater salinity due to the presence of the ice crystals; Onstott *et al.* (1998) measured the salinity of grease ice to about 20 psu. Pancake ice is formed in a frazil ice cover suspended in a wave field. The frazil ice layer is subject to cyclic compression by the waves. During compression crystals freeze together to form the initial aggregates that later become floes. Wave energy is sufficient to prevent the frazil ice or water between the pancake floes to consolidate or freeze and further to wash material onto and compress the floe by collisions as part of the special growth process (e.g. Weeks & Ackley, 1986; Wadhams, 2000; Shen *et al*., 2001). Ice floe cover concentration has been reported in belts to 20-30 %, and in a dense pancake field: ~70 % (Wadhams *et al*., 1996) and ~85 % (Comiso *et al*., 1989). The pancake growth rate is a function of the supply of frazil, air temperature and turbulence level (Shen *et al*., 2001). The maximum potential pancake size decreases as a function of ocean wave amplitude and increases as a function of ocean wavelength (Shen *et al*., 2001). Individual pancake floes are typically up to 2 – 3 m in diameter (Wadhams *et al*., 1996). Pancake ice is usually not snow covered. The surface roughness of a pancake ice cover is very different for pancake ice at different stages of development and formation environment (Tucker *et al*., 1991; Onstott *et al*., 1998). The rims form the major roughness elements on the floe (Dierking, 2001). The rim height is related to the supply of frazil ice, pumped onto the floe by collisions (Shen *et al*., 2001). Onstott *et al*. (1998) measured the surface roughness of pancake floes formed in a wave tank experiment. The floes were about 30 cm in diameter and the root-mean-square roughness of the floe was 0.018 - 0.506 cm and correlation length 0.74 – 2.765 cm. The salinity profile of two 14 hours old pancake floes measured by Onstott *et al*. (1998) in different sections of the floes was between 9-15 psu. Tucker *et al*. (1991) measured the salinity of pancakes in the Fram Strait from 9-12 psu. Wadhams *et al*. (1996) measured very low salinities of pancakes in the Greenland Sea down to 2 psu but also more normal salinities for this ice type around 12 psu. Further in the Greenland Sea salinities of pancakes was measured to between 4-21

psu (CONVECTION, 2001). Tucker measured the density of pancake ice to 920 kg / m^3. Pancakes normally have a hard top and soft bottom, due to adhesive freezing of the free-board.
Freezing under calm conditions creates nilas, which is a smooth elastic ice cover < 10 cm thick. Its growth is determined by both thermodynamic growth and rafting (Tucker *et al.*, 1991). The crystal structure is in general preceding the growth of columnar first-year ice. The salinity of nilas measured in the Fram Strait is 14-16 psu and the density about 920 kg/m^3 (Tucker *et al.*, 1991). The major roughness elements on the nilas surface are edges created by over-thrusting (Tucker *et al.*, 1991) and frost flower formation (Grenfell *et al.*, 1992; Onstott, 1992; Ulander *et al.*, 1995). Grease ice, pancake ice and nilas are all new-ice types which are per definition <10 cm thick. This does however not mean that pancakes or grease ice cannot grow thicker than 10 cm and still be new-ice. The character and stage of development of the ice must be considered before classification.

Processes and properties of mature sea ice

Young ice, which is 10–30 cm thick consolidated ice, is formed by continued freezing of new-ice formed under calm or turbulent conditions. The continued ice thickness growth of un-deformed young ice is thermodynamic rather than thermodynamic-mechanical. The continued thermodynamic growth of the ice is by constitutional super cooling (CSC). The CSC growth process is important for the initial entrapment of brine. The concentration of salt in the water below the ice is increasing towards the ice interface due to brine expulsion during ice formation. The salinity profile creates a zone just beneath the ice where the actual temperature is below the equilibrium freezing temperature and the water is therefore super-cooled. The super-cooling makes the ice grow in cells and brine is trapped in grooves between these cells. The faster the growth rate, the smaller is the brine layer spacing. Typical layer spacing is 0.5 – 1 mm for growth rates of 1– 2 cm/day (Weeks & Ackley, 1986). Ice grown faster contains more brine. The liquid brine trapped in the ice is contained in brine pockets. The volume of liquid brine in a given sample of sea ice is a function of ice salinity and ice temperature. Salts in brine start freezing at particular temperatures, e.g. mirabilite ($NaSO_4$ $10H_2O$) at -8.2˚C and hydrohalite (NaCl $2H_2O$) at -22.9˚C (Light *et al.*, 2003).

Two types of crystal structure is characterising frazil or columnar first-year ice. Turbulent mixing of crystals before consolidation generates frazil ice. Columnar ice is formed by geometric selection: the maximum growth rate of the ice crystal is in the basal plane; crystals oriented with the basal plane vertically will have the fastest and most unrestricted growth. The fast growing crystals eventually dominate the ice growth at the subsurface, i.e. the crystals with the a-plane parallel to the growth direction. Un-deformed first-year ice is 30 – 200 cm thick. Ice surviving the seasonal melt is called multiyear ice. Multiyear ice is usually thicker than 200 cm. The crystals in multiyear ice are re-crystallised in connection with the summer surface melt and freeze-up and therefore not related to the initial ice formation process. Multiyear ice is characterised by a rolling, hummocky surface, which is the result of differential melt (Weeks & Ackley, 1986). The salinity is increasing downwards with about 0.0 – 0.1 psu above sea level and 3.0 – 3.5 psu below. Multiyear hummocks are often characterised by a low-density upper layer and more dense ice below. The air bubble radius in multiyear ice is typically < 5 mm in diameter. The surface of a hummock is rough and porous and melt-ponds are relatively smooth and have higher density (Onstott, 1992). The surface roughness is defined according to the standard deviation of the surface height, σ_{RMS}, and the surface correlation length, L (Ulaby *et al.*, 1981). Measurements of ice surface roughness are plotted in terms of these two roughness parameters in figure 1. Table 1 is showing the air-bubble size, density and salinity of sea ice. The measurements in table 1 are from field and laboratory experiments.

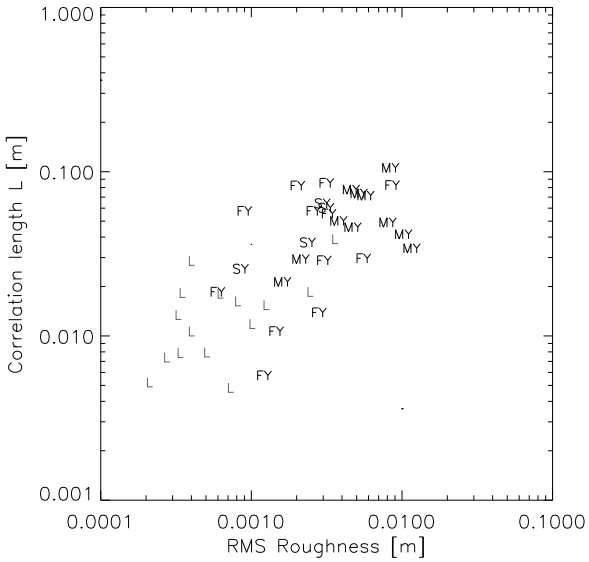

Figure 1. First-year (FY), second-year (SY), and multiyear (MY) ice surface roughness reported from Arctic field experiments in: Onstott, (1992); Carlström *et al*., (1993); Dierking *et al*., (1999); Nghiem *et al*., (1995) and laboratory studies (L): Beaven *et al*. (1995); Bredow & Gogineni, (1990); Onstott, (1992).

	FY upper layer	FY lower	MY upper layer	MY lower
Thickness [m]	0-0.36 [1]	<2	0.03-0.22 [2,4]	>2
Density [kg/m^3]	800-920 [1,3]	870-920 [3]	457-914 [4]	870-920 [6]
Salinity [ppt]	5.1-11.9 [1,5]	5.1-11.9 [1,5]	0.0-0.8 [5]	0.1-3.0 [6]
Air bubble size [mm]	0.1-2.5 [3]	0.1-2.5 [3]	<2.5 [5]	<2.5 [5]

Table 1. Observed Arctic ice properties in: 1) Campbell *et al*. (1978), 2) Carlström *et al*. (1993), 3) Dierking *et al*. (1999), 4) Onstott (1992), 5) Shokr (1998), and 6) Winebrenner *et al*. (1992). The super-script indicates these six references. The first-year (FY) and multiyear (MY) ice properties are ordered in an upper surface layer and a lower ice profile beneath.

One of the important differences between first-year ice and multiyear ice is the salinity profile. The salinity of sea ice is determined by 5 different processes: 1) the initial amount of salt entrapped in the ice, 2) the migration of liquid inclusions through the ice, 3) brine expulsion or squeezing of brine out of the ice as a result of differential volume changes in the different phases composing the sea ice, 4) brine gravity drainage, and 5) flushing. The primary brine drainage mechanism in winter is by brine gravity draining through a structure of channels. Ice grown at faster rate has more channels. Flushing is when the drainage channels are flushed by water, in particular melt water during summer. Flushing is the most significant sea ice salt depletion process (Weeks & Ackley, 1986).

Processes and properties of snow

The range of mean snow depth in winter (Nov. – Feb.) over the Arctic Ocean varies from a maximum value north of Greenland to a double minimum in Laptev and Beafort Seas. In spring (Mar. – Apr.), the maximum snow depth shift to the Fram Strait (Arctic Climatology Project, 2000).

In spring before melt the snow thickness on sea ice is 20 – 30 cm in the Greenland and Barents Seas (Garrity, 1992), ~ 15 cm in the Labrador Sea (Drinkwater, 1989) and 10 – 15 cm for the Arctic sea ice in general (Tucker *et al*., 1992). Larger snow depth are not unusual; e.g. in the Lincoln sea snow depth between 40-70 cm was usual during the field campaign 2006. The average snow density increases throughout the snow accumulation season from 250 kg/m^3 in September to 320 kg/m^3 in May, averaging

300 kg/m^3, with little geographical variation (Warren *et al*. 1999). The snow pack insulates the ice surface against the cold or warm atmosphere with a heat conduction coefficient of ~0.3 W/mK compared to e.g. ~2.1 W/mK for sea ice (Maykut, 1986). The σ_0 and Tb are both directly affected by the snow properties e.g. liquid water content, grains size, density etc. and indirectly by the thermodynamic control of the snow cover on the ice e.g. ice brine volume (Barber *et al*., 1995). The relatively thin snow cover in the Arctic Ocean can give large temperature gradients within the snow. A strong temperature gradient and the resulting vapour flux forms depth hoar crystals (see picture) of 2 – 5 mm in diameter at the snow-ice interface or near the snow surface (Garrity, 1992; Amstrong *et al*., 1993; Colbeck, 1989; Colbeck, 1990). The snow grain size is important for the brightness temperature and the spectral gradient ($Tb_{19H} - Tb_{37H}$) (Josberger & Mognard, 2002). The spectral gradient is a measure of Tb measured at different frequency bands.

Photo 2. Skeleton depth hoar crystals, the tube is 5 cm in diameter.

Thermal conductivity of sea ice

The thermal conductivity of sea ice shown in figure 2 is dependent both on ice salinity and temperature.

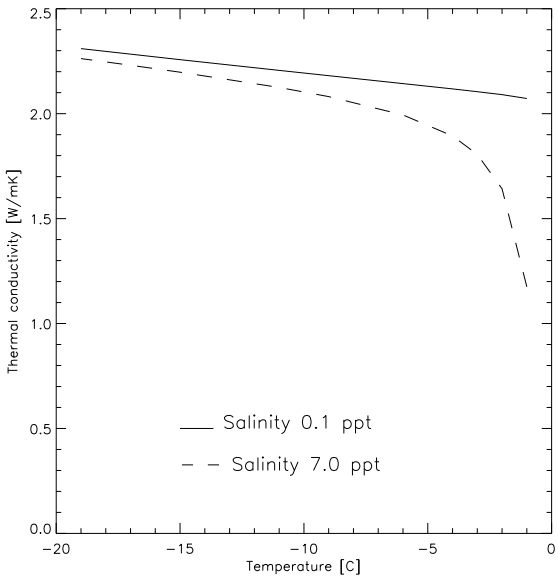

Figure 2. The thermal conductivity of first-year and multiyear sea ice.

Figure 2 show that for temperatures about < -5˚C the thermal conductivity (k_i) is nearly constant. A typical value for k_i is 2.1 W/mK (Maykut, 1986). The thermal conductivity of snow (k_s) is much lower namely 0.31 W/mK (Maykut, 1986). The ice and snow temperature profile are roughly linear (Nakawo & Sinha, 1981). When the top and bottom temperatures (T) of the ice or snow are known the temperature at some depth (d) within the ice can be found using the temperature gradient, i.e.

$$\frac{\partial T}{\partial z} \approx \frac{T_{bottom} - T_{top}}{d} \qquad (1).$$

The typical values, mentioned above, for the thermal conductivity (k) of ice and snow can be used to compute the snow/ice interface temperature for different air temperatures and snow and ice thickness using equation 2 below, where the subscripts w, a, s and i indicate water, air, snow, and ice respectively. T, is the temperature, k, the thermal conductivity and d the layer thickness.

$$T_{si} = \frac{T_w + fT_a}{f+1},\ f = \frac{k_s d_i}{k_i d_s} \qquad (2).$$

Air temperature[C]		-5			-20			-30		
Snow thickness [m]		0.05	0.1	0.2	0.05	0.1	0.2	0.05	0.1	0.2
Ice thickness [m]	0.3	-2.9	-2.2	-1.7	-9.9	-6.8	-4.4	-14.6	-9.9	-6.3
	0.5	-3.4	-2.7	-2.1	-12.3	-9.1	-6.1	-18.3	-13.3	-8.8
	1.0	-4.0	-3.4	-2.7	-15.2	-12.3	-9.1	-22.6	-18.3	-13.3
	2.0	-4.4	-4.0	-3.4	-17.2	-15.2	-12.3	-25.8	-22.7	-18.3

Table 2. The snow ice temperature computed using equation 3.4 and the thermal conductivity 0.3 W/mK and 2.1 W/mK for snow and ice respectively.

Microwave interaction with snow and sea ice

The permittivity (ε) of snow is determined by its density and liquid water content (Ulaby *et al.*, 1986). The permittivity of snow is affecting the reflection, transmission and the absorption coefficients. Scattering in the snow pack is detectable for frequencies higher than 10 GHz (Barber *et al.*, 1998) and is important for coarse snow grains or high frequency (ν > 20 GHz) (Mätzler, 1987). The permittivity of sea ice is largely given by the brine and air-inclusion volume (Shokr, 1998). Surface scattering is a function of the roughness scaled to the wavelength and the reflection coefficient. Important for volume scattering in sea ice is the size and number density of brine pockets or air bubbles (Winebrenner *et al.*, 1992).

Permittivity models for snow and ice

Most of the dielectric mixing models for snow and ice in the literature are based on the work of Polder & Van Santen (1946). The permittivity, ε (ε = ε’ + jε’’), is defined by its real part (ε’) and its imaginary part, the loss (ε’’) (Hallikainen & Winebrenner, 1992).

Dry snow

The ε’ of dry snow is nearly independent of temperature and electromagnetic frequency. It is here given as a function of snow density, ρ (Ulaby *et al.* 1986), i.e.

$$\varepsilon'_{ds} = (1 + 0.51\rho_s)^3 \qquad (3).$$

This relation gives excellent fit to data (Ulaby *et al*., 1986).

The ε'' is in Hallikainen *et al*. (1986) modelled using a Polder & Van Santen formula where the snow particles are spheres of ice embedded in air. Equation 4 gives a good fit to data (Hallikainen *et al*. 1986). The loss, ε'', is found simplifying the equation by ignoring insignificant contributions whenever appropriate i.e.

$$\varepsilon''_{ds} = 3v_i\varepsilon''_i \frac{\left(\varepsilon'_{ds}\right)^2\left(2\varepsilon'_{ds}+1\right)}{\left(\varepsilon'_i + 2\varepsilon'_{ds}\right)\left(\varepsilon'_{ds} + 2\left(\varepsilon'_{ds}\right)^2\right)} \qquad (4).$$

The ε is the permittivity and v is the volume fraction of ice spheres. Subscripts i denote ice and ds; dry snow.

Wet snow
The ε of water is an order of magnitude larger than ε of pure ice. The ε of wet snow is therefore primarily a function of volumetric water content.

Permittivity models for sea ice

The ε of sea ice is primarily a function of brine volume. The brine volume is dependent on the ice salinity and the temperature. For example, Vant *et al*. (1974) and Vant *et al*. (1978) derived empirical models (10 GHz) for the ε of sea ice only as a function of brine volume, v_b e.g.

$$\varepsilon'_{columnar} = -0.377 + 3.498\left(\frac{1}{1-3v_b}\right)$$
$$\varepsilon''_{columnar} = 0.004 + 7.143v_b \qquad (5),$$

and for first-year ice (4 GHz) (Vant *et al*., 1978), i.e.

$$\varepsilon'_{si} = 3.05 + 0.72v_b$$
$$\varepsilon''_{si} = 0.024 + 0.329v_b \qquad (6).$$

The Vant *et al*. (1974 & 1978) models are empirical modifications of the model by Hoekstra & Cappillino (1971). The latter derived a simplified Polder & Van Santen formula for spherical brine inclusions for ε' and a mixing formula for ε'' (Hoekstra & Cappillino, 1971), i.e.

$$\varepsilon'_{si} \cong \frac{\varepsilon'_i}{1-3v_b}$$
$$\varepsilon''_{si} \cong v_b\varepsilon''_b \qquad (7).$$

However, the ε of sea ice is also a function of e.g. the volume of air included in the ice, the frequency and the scattering. In general, the permittivity of a mixture, ε_m, is a function of the volume fraction and the shape and distribution of the inclusions. The appropriate model to use is dependent on the ice type and structure (Vant *et al*., 1974; Shokr, 1998). The recommendations of Shokr (1998) are summarized in table

3.

Ice type	Model type
First-year frazil ice	Randomly oriented brine needles in pure ice
First-year columnar ice	Vertically oriented brine needles in pure ice
Multiyear hummock	Any shape of air inclusions in pure ice
Pond ice	Vertically oriented brine needles and spherical air bubbles

Table 3. The appropriate model for different ice types according to Shokr (1998).

Permittivity of brine

The volume fraction and the permittivity of brine are important for the dielectric properties of sea ice. In order to compute the dielectric properties of brine one must first compute properties only indirectly related to its permittivity. The salinity of brine is related to the ice temperature. The normality of the brine solution is related to the brine salinity. Properties determining the dielectric properties of brine like relaxation time of the solution and the conductivity are related to the temperature and the normality. The permittivity of brine is a function of frequency, relaxation time, static dielectric constant, and conductivity (Ulaby *et al*. 1986).

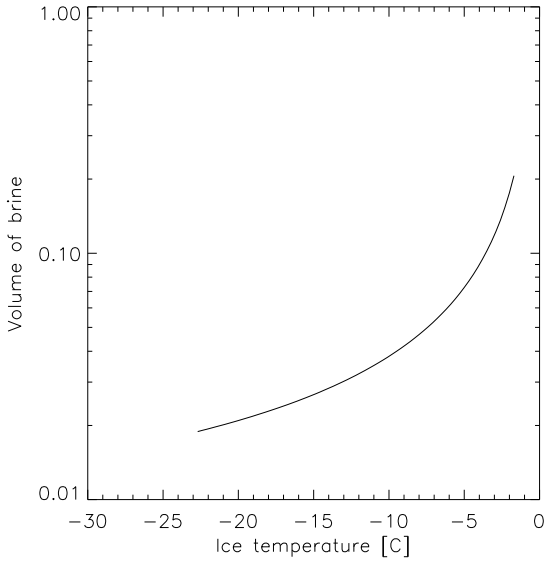

Figure 3. The volume of brine in sea ice with salinity of 7 psu.

Reflectivity, transmissivity and surface scattering

The reflectivity, r, at the boundary between medium 1 and 2 is

$$r = \frac{n_1 - n_2}{n_1 + n_2} \qquad (8),$$

where the refractive index is the square-root of the permittivity, i.e. $n = \sqrt{\varepsilon}$. The reflectivity and the tranmissivity are related, i.e. | t |+| r |=1. The transmission angle is given by the law of Snellius.

Surface scattering in radar applications is approximated using for example the integral equation method (IEM), geometric optics etc. (Fung, 1994) and for nadir scattering (altimeter) models described in e.g.

Fetterer *et al*. (1992).

The reflectivity and transmissivity between the natural layers in the snow-ice system are important for the microwave polarisation at oblique incidence angles and surface scattering is a function of the reflectivity, roughness and incidence angle, i.e. the geometrical optics model,

$$\sigma^0 = |R(0)|^2 \frac{\exp\left(-\frac{\tan^2\theta}{2m^2}\right)}{2m^2\cos^4\theta} \qquad (9),$$

where m is the roughness slope, for Gaussian roughness distribution, $m = \sqrt{2}rms/l$, *R(0)* the reflection coefficient at normal incidence and θ the incidence angle.

Extinction and volume scattering

The extinction, e, is the sum of scattering, s, and absorption, a, i.e. e = σ + a. The absorption is primarily a function of the dielectric loss, ε'' and wavelength, λ. The penetration depth in a non-scattering dielectric is:

$$pd \approx \frac{\lambda}{2\pi}\frac{\sqrt{\varepsilon'}}{\varepsilon''} \qquad (10).$$

The volume scattering is described by e.g. the improved Born approximation (Mätzler, 1998), i.e.

$$\sigma_{vol} \cong \frac{3p_{ec}^3k^4}{32}v(1-v)\left|\frac{(\varepsilon_2-\varepsilon_1)(2\varepsilon_{eff}+\varepsilon_1)}{2\varepsilon_{eff}+\varepsilon_2}\right|^2 \qquad (11),$$

where p_{ec} is the correlation length, a measure of scatterer size, k the wavenumber, ν the volume fraction of scatterers and ε_1, ε_2, ε_{eff} is the permittivity of the background, the scatterers and the layer, respectively. A description of the volume scattering coefficient such as the improved Born approximation is appropriate for snow and sea ice.

Microwave radars and radiometers

Radar altimeters

Nadir looking Ku-band radar backscatter is dominated by (smooth) surface scattering processes, i.e. the snow and ice surface. Volume scattering may contribute to the extinction in the snow cover and thereby the distribution of scattering magnitude between the snow and ice surface and the total scattering magnitude, but volume scattering is negligible as a source of backscatter. Absorption in the snow layer may be significant if it is moist or saline.

Active microwave side-looking instruments: scatterometer, SAR, SLAR

C-band radar backscatter at oblique incidence angles is primarily a function of surface scattering processes. The volume backscatter contribution, especially from multiyear ice, is not negligible. In X and Ku-band both surface and volume scattering processes are important for the total backscatter coefficient.

Passive microwave radiometer instruments

Microwave radiometers measure spectrally at different polarisations. The radiation intensity is related to reflectivity and extinction and unlike radar; the surface scattering is in most cases negligible. The application of these data range from atmospheric sounding to sea ice concentration mapping. The later using the

polarisation and spectral gradient is in particular sensitive to variations in sea ice reflectivity and scattering.

Microphysical snow and sea ice measurements

In the following, simple procedures are described for sampling the most important microphysical parameters for microwave remote sensing data analysis over snow covered surfaces. These microphysical parameters are important for the permittivity, reflectivity and scattering of microwaves of sea ice as describe above. The microphysical measurements should be made in the following order:

1. Detecting horizontal snow layers.
2. Snow temperature.
3. Hardness of the layer
4. Grain size and shape.
5. Snow density.
6. Salinity samples.
7. Surface roughness.
8. Ice salinity coring.

Photo 3.Ice thickness and freeboard measurements, North of Alert, Arctic Ocean.

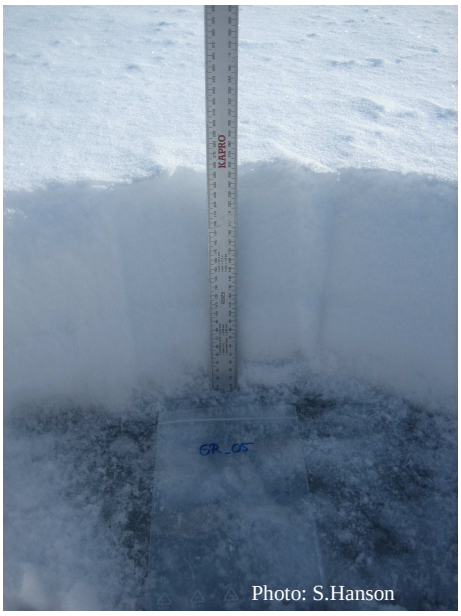

Photo 4. Snow profile on FYI sea ice, North of Alert, Arctic Ocean.

Snow and ice sampling

Warren *et al*. (1999) argue that snow measurements 10 m apart are in fact independent and that 5 samples gives a standard deviation of 2 – 7 cm of the mean thickness, 50 samples 1.8–2.3 cm and 100 samples 1.3–1.6 cm. When doing coincident *in situ* snow/ice and microwave measurements it is noted that independent snow samples are only 10 m apart.
In the same way drilling one borehole will determine mean ice thickness with ± 0.5 m. Drilling 50 boreholes 1 km apart will make the samples independent and reduce the standard deviation to 0.33m. The variance of the thickness estimate is the variance of the thickness distribution divided by the number of independent samples (Rothrock, 1986).
At the Russian Arctic drift-stations snow depth is to be measured daily at three stakes (25 m apart) enclosing the meteorological station and furthermore for every 10 m along 500 – 1000 m snowlines.
If samples are taken over longer time; weeks/seasonal, it is necessary to establish a sampling area on a level and homogeneous floe (see map). In DAMOCLES the following sample method has been determined:
Snow pits are to be measured weekly at three stakes (25 m apart) and furthermore for every 50 m along a 150 m snowlines (3 pits per line, 9 all in all). During the melt period (1st of April) once a day until snow is melted away.
Conductivity of melted snow and ice surface samples are needed once every week.
Ice thickness and **freeboard** should be done as well every week. These should be done along the same line but for every 10 m (15 per line, 45 all in all).

After a snow pit or ice thickness measurements the hole should be covered carefully and marked to avoid using the same spot twice. The following week all 3 lines are moved 1m to the side and the procedure is repeated. If not enough space the sampling site will have to be moved to a new floe.

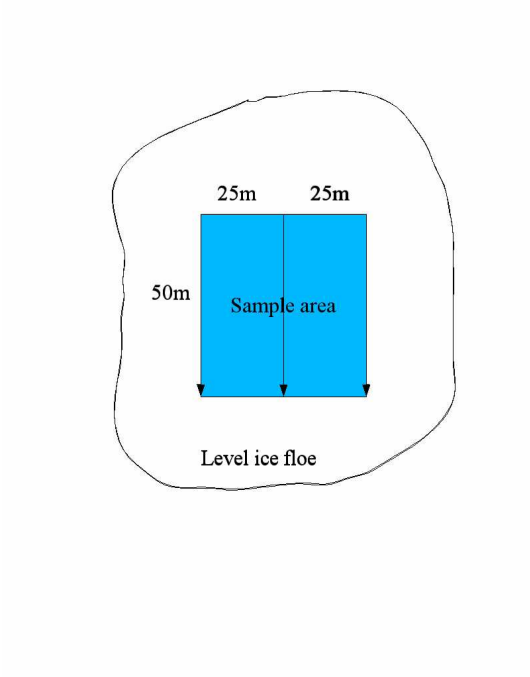

Figure 4 Profiles are spaced 10 m (ice thickness) or 50 m (snow pits) apart along each of the 3 arrows at regular intervals e.g. each week. It is important to cover the hole and level the snow after measurements.

General description

At each snow pit note the following to begin with. When returning to the office the data is saved in the electronically snow pit scheme (Figure 5)

- Date, time, observer, location, GPS position
- Air temperature, cloud cover fraction, precipitation and wind.
- Note the maximum surface roughness with in a meter and within 10 meter.
- Make sure the wall of the snow pit is vertical, clean and as smooth as possible and is facing North.
- Take a picture of the snow pit with the rule up against the snow wall, 0 is at the ice-snow interface (Photo 4) and insert this later in the electronically snow scheme.

The snow surface and roughness

A precise description of the snow surface is important to understand the response of the microwave to the snow and give a first impression of the snow pack.
Please note:

- Is there new fallen snow? depth hoar? whole new-snow crystals?
- Is it wind packed?
- Does it have a glance?
- Is it the bare ice-surface?
- Take a picture using the ‘surface-scale-frame’

The surface roughness is very important dealing with microwave measurements and therefore an estimate of the ‘true’ roughness of the snow and ice surfaces is essential. Template devices, stereo photography, laser profilometers and surveying have been used to quantify surface roughness (Dierking, 1999). A more elaborate discussion of sea ice roughness measurements is given by Dierking *et al*. (1997).
The devices mentioned above are difficult to use in the field. Alternatively estimate of the microscopic and macroscopic roughness visually, i.e. magnitude of height undulations across 1m and across 10 m.

Identify Layer thickness

When the snow pit has been dug, begin with a measuring of the full depth and mark it in your notebook (Photo 4). The boundary between each layer is measured from the ice surface at the bottom of the snow pack. Start by letting one finger run over the profile from bottom to top. Then it is pretty easy to distinguish the individual layers by the difference in consistency and resistance of each layer. The thickness of each distinct layer is marked in the snow chart and used in the further description of the profile.

Thermometric temperature

Measure the temperature at the snow-ice interface at the bottom of the snow pack (the so called BTS temperature) and the temperature at the snow-air interface, in such a way that the 'arm' of the thermometer is just covered. Remember to cover the surface to avoid heating of the 'arm' by the sun – use the spade. This temperature is not necessarily the same as the air temperature. The snow-air and the snow-ice interface temperatures are of particular importance. The temperature measurements provide a thermal profile, which is necessary to provide an understanding of the metamorphic changes taking place in the snow pack.
Now, measure the temperature in the middle of each individual layer. If no layers can be recognized do the measurements at regular intervals, normally for every 5 cm.

Description of the individual layers

Once snow falls to the ground it will soon undergo processes where it changes its original shape whereby the texture of the layer changes as well. This is important for the structural strength, permeability, thermal conductivity and density of the snow layer.
The snow grain size and shape should be estimated together with the hardness in every single layer.
The hardness measurements of the individual layers are subjective. One should try to use the same force each time when using the so called 'hand test'. With the hand test, objects of different areas are gently pushed into the snow with a penetration force of about 50 N, which is easily executed with hand. This hardness of the individual layers are basic when the snow pit scheme is drawn (figure 5 and 'pit_instructions_Damocles.xls').

Term	Swiss Rammsonde (N)	Hand test
Very low	0-20	fist
Low	20-150	4 fingers
Medium	150-500	1 finger
High	500-1000	pencil
Very high	> 1000	knife
ice		

Table 4. Snow hardness.

The ice surface (below the snow) should be described including visible brine pocket and bubble size.

Estimation of snow grain size and shape

Observations of grain size and shape should be done in each distinct layer. Grain size is taken as the maximum dimension of a single grain or crystal. Grain fragments must not be mistaken for individual grains. A snow crystal screen is a coloured chart covered by a mm grid pattern. Throw a small amount of snow on the card and note down the size of grains (e.g. < 5 mm, 1-2 mm) (Photo 5, 6). In the case of extreme bonding (e.g. ice layer) or in very wet snow, grain size and shape lose their meaning and need

not be recorded. Take two pictures with the layer code (like 2-22 cm) and insert this later in the electronically snow scheme. It is quick and gives a reasonable idea for the later users of the data.

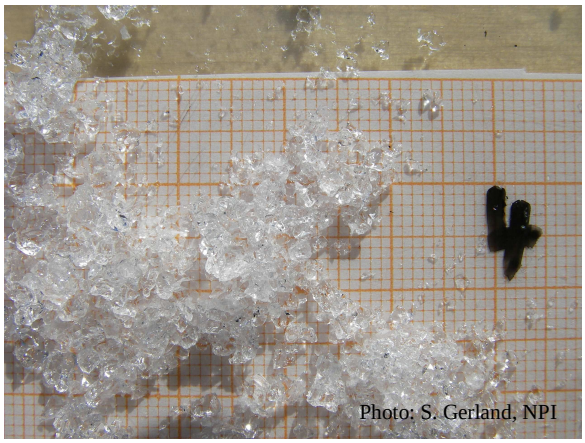

Photo 5 and 6. Snow crystals on snow card

Snow undergoes several mechanical and physical processes that will change the shape of the grain in an ongoing progression. Snow undergoes two main processes of metamorphoses: the equi-temperature metamorphism, which is a natural rounding of the individual grains due to internal vapour pressure differences within the single grain, and the temperature gradient metamorphism which is due to the vapour gradient within the snow pack created by the temperature gradient. Furthermore the single grains can break down during under the force of wind, or ongoing melt and freeze will reshape the grains. For a fully correct classification please see 'The International Classification for Seasonal Snow on the Ground'. When dealing with scattering and penetration of microwaves in snow it is mainly the shape (and no so much the process) of the individual grains that are of interest. The classification of snow in this context is therefore strongly simplified. The main grain shapes are described below. Record the appropriate signature on the data sheet. Note that, often a transition between two main classes is found. If this is the case note down that a transition between two main classes are found e.g. rounded grains plus beginning depth hoar. Further classes with belonging sub-classes are described in 'The International Classification for Seasonal Snow on the Ground'.

Precipitation particles (signature: +)
This type refers to freshly deposited snow composed mainly of whole crystals or parts of broken ones. All the grains have individual characters. The snow is usually very light and the layer pan be punctured by a finger.

Fragmented crystals (signature: /)
This type of snow is composed mainly of fragments of crystals and refers to snow during the initial stage of rounding of the original or wind broken particles while the snow is still dry the. Although it has lost a great deal of its crystalline character, some crystalline features can be observed; it still sparkles. The snow is usually fairly light.

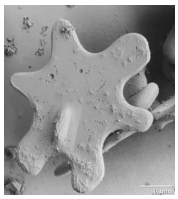

Rounded grains (signature ●)
When snow is transformed by metamorphism, it completely looses all crystalline features and its grains become irregular or more or less rounded. It has no sparkle effect even in bright sunlight and can readily be recognized by its dull appearance. It is usually fairly soft when wet, but can be very hard when frozen (sometimes you will need a knife to penetrate the layer). This type of snow grains may be any size from very fine to very coarse. If pellets or hail is present it should be noted whengiven the same signature.

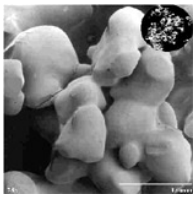

Faceted crystals (signature /)
At temperatures well below freezing and without any apparent melting, crystals are formed by deposition of water vapour removed from crystals deeper in the profile (sublimation). Deposition produces irregular grains with flat facets. These facets are visible with a lens and give the snow a distinct sparkle effect in the bright sunlight. The layer is often only a few millimetres thick and can be fairly hard.

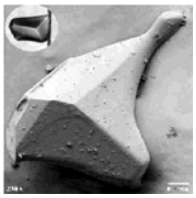

Depth Hoar (signature ^)
Depth hoar is characterized by its hollow cup-shaped crystals and is very easy to recognize. These crystals (0.5 cm – 2 cm) are produced by a very low rate of deposition of sublimed vapour during a long uninterrupted cold period. Depth hoar is most frequently found directly below a more or less impermeable crust in the lower part of the snow covers. The tensile strength of a layer of depth hoar is very low and the structure of the layer falls away at the slightest touch.

On multi year ice the structure of last years weathered summer surface can easily be mistaken for depth hoar. Normally the weathered summer surface can be distinguished from depth hoar by that the first will have a skeletal structure compared to the VERY loose structure of depth hoar.

Density measurements

When doing the density measurements start from the top of the snow pit and do one measurement of each layer thicker than 5 cm. If you have a very distinct thin layer, like a thin ice lens between two soft layers,

a sample can be taken where the thin layer is in the bottom of the uppermost soft layer. The uppermost layer has to be measured separately as well of course.

1. Position cutter perpendicular to wall of the snow pit in both vertical and horizontal directions.
2. Hold cutter in place with one hand while inserting cutter lid in with the other.
3. In consolidated or wet snow, once the lid is pressed in and the sample has been isolated, the cutter and sample may be removed and weighted while the lid is left in. In new, unconsolidated, weak, or kinetic (depth hoar) snow, the lid should be removed from the pit wall with the cutter to insure no sample loss. In extremely dense snow, refrozen melt-freeze or thick ice lenses it may be necessary to use a rubber mallet to insert both the cutter and the lid. Both parts are strong enough to use in this manner if done with care. Do not hit cutter handle with mallet. Hit lower corners of the cutter. Do not use anything except a rubber mallet. In conditions where sticking or icing make sample removal difficult, a putty knife may be helpful. Be sure that the snow is not compressed during the measurements and, at the same time, that the container is completely filled.
4. Transfer the snow sampler to the digital scale or to a bag and weight the bag with the spring scale (remember to weight the cutter or bag alone first so its weight can be subtracted from the total weight)

Ice samples diameter and length of ice core sections are measured with ruler and the sample is weighted. The sample is collected for later estimation of salinity.


Photo.: S.Hanson

Photo.: S. Gerland, NPI.

Photo 7.

Salinity

Collected samples from the snow density cutter can be used for salinity estimation in the laboratory. The salinity is a function of electric conductivity and temperature (and pressure). The salinity scale is defined according to conductivity (Fofonoff, 1985). Temperature and conductivity are measured in melted samples with a conductivity meter. The absolute conductivity reading is converted to salinity using the formulation for seawater in Fofonoff (1985). For example, the matlab code is found in (http://woodshole.er.usgs.gov/operations/sea-mat/omviz-html/swstate.html). Dilution of the sample may be necessary in the laboratory to obtain sufficient sample size or for very saline samples (beyond conductivity meter scale).

When determine the salinity, collect the snow from the scoop in a plastic bag, when the weight for the density measurements have been noted down. Note the layer from which it is taken and bring the bag back to melt the snow. When the snow is melted measure the conductivity using the conductivity meter. Note that the probe must not be flushed with freshwater between snow samples, and between ice samples, but after a snow sample set and after an ice sample set of samples (and certainly before storage). It has to be checked if the conductivity meter is temperature compensated. The conductivity should be noted in the snow pit scheme for each layer.

Liquid water content

The water content can be measured with a snow fork if the snow is not saline. It is generally a problem to measure liquid water content in snow, which is potentially saline. Alternatively, the snow should be classified as dry, moist, wet, and saturated.

Sea ice measurements

Ice thickness measurements are easily done by removing the snow layer and drill through the ice with the special equipment made to attach to a perfectly normal drilling machine. The drilling it self take not more than a few minutes. The ice auger flights are 5 cm in diameter, 1 m long and join one to another via a patented push-button connector, which allows for quick connection of one auger section to another. This method of assembly means that there are no pins or connector bolts to lose or care for and no bolts on which clothing can snag. When inserting a new flight be careful, that one is holding onto the flights in the ice while the drilling machine is lifted of to avoid the remaining flight to be dropped in the ocean.
An adapter is required for turning the augers using a 1/2 inch (1.5 cm) electric drill. It is strongly recommended to powering the flights with a heavy duty electric drill rated at 550 to 650 RPM. Drilling rates of 1 m in 15 seconds in ice are achievable with this mode of power drive. The bits should be sharpened by hand filing once in a while.
When the hole is drilled, drop the ‘UEDA thickness gauge’ through the borehole. This device when lowered through a borehole and then pulled upward will bridge across the hole at the bottom of the ice. The support measurement tape is then read to provide the ice thickness (photo 1). A tug on the tape then collapses the gauge for retrieval. It is important to check regularly the small screw on the thickness gauge. If a screw is loose one can loose a part of the system. Here, also the folding strength can be adjusted. If it is cold (and one measures in a 5 cm auger hole), one should not adjust it very hard, otherwise the tape measure may break and the gauge would be lost.
With the folding ruler measure the difference between the ice surface (not the snow surface) and the water level in the borehole. This is the so called freeboard.
Total snow depth, ice thickness and freeboard are noted down in the snow pit scheme.

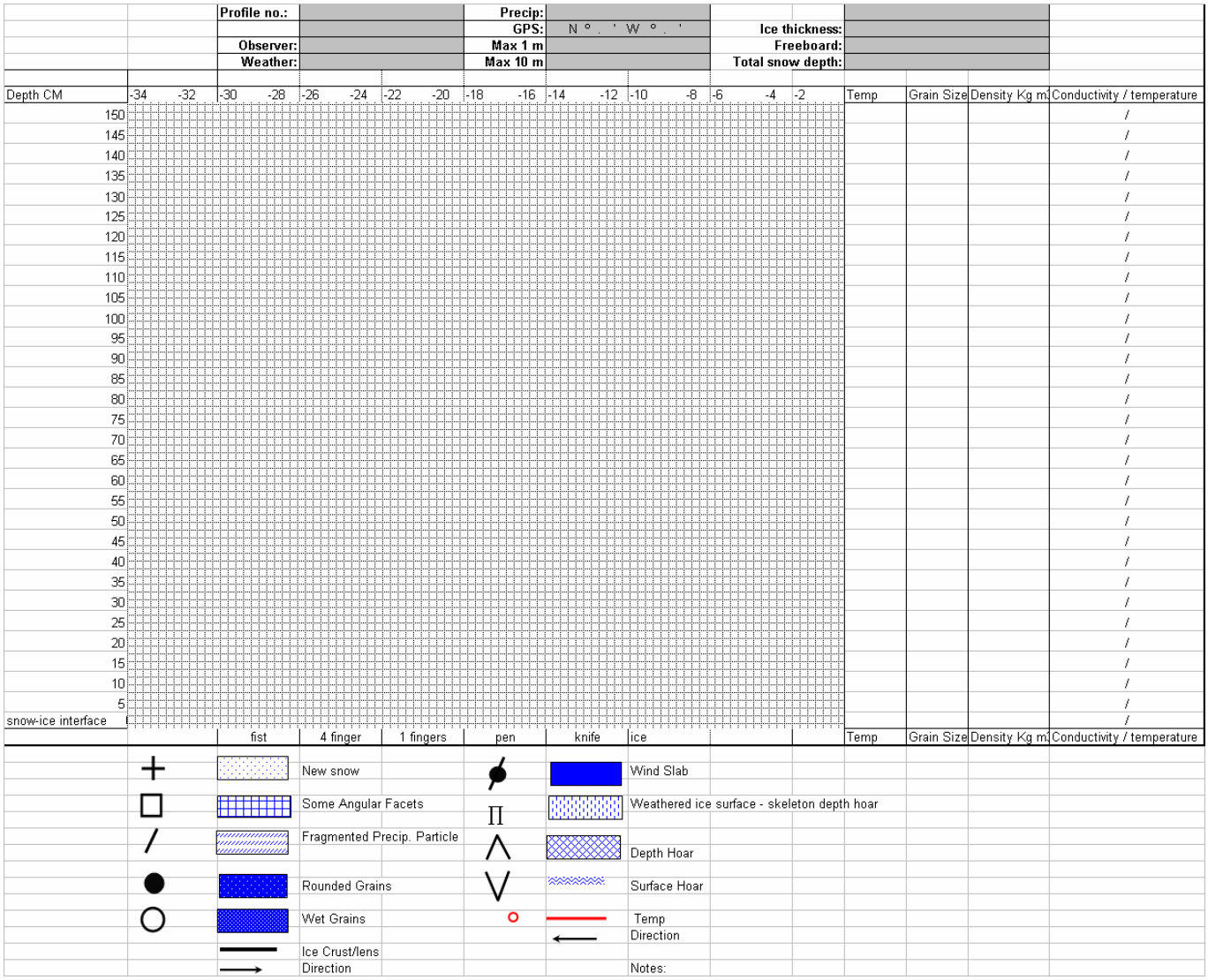

Figure 5. The electronically snow chart developed for use at the DAMOCLES project for the crew on TARA.

References

Arctic Climatology Project (2000). Environmental Working Group Arctic Meteorology and Climate Atlas. Edited by F. Fetterer and V. Radionov. Boulder, CO: National Snow and Ice Data Center. CD-ROM.

Armstrong, R. L., A. Chang, A. Rango, E. Josberger (1993). Snow depth and grain-size relationships with relevance for passive microwave studies. *Annals of Glaciology 17*, 171-176.

Barber, D. G., A. K. Fung, T. C. Grenfell, S. V. Nghiem, R. G. Onstott, V. I. Lytle, D. K. Perovich, & A. J. Gow (1998). The role of snow on microwave emission and scattering over first-year sea ice. *IEEE Transactions on Geoscience and Remote Sensing 36*(5), 1750-1763.

Barber, D. G., S. P. Reddan & E. F. LeDrew (1995). Statistical characterisation of the geophysical and electrical properties of snow on landfast first-year sea ice. *Journal of Geophysical Research, 100*(C2), 2673-2686.

Beaven, S. G., G. L. Lockhart, S. P. Gogineni, A. R. Hosseinmostafa, K. Jezek, A. J. Gow, D. K. Perovich, A. K. Fung, & S. Tjuatja (1995). Laboratory measurements of radar backscatter from bare and snow-covered saline ice sheets. *International Journal of Remote Sensing 16*(5), 851-876.

Bredow, J. W., & S. Gogineni (1990). Comparison of measurements and theory for backscatter from bare and snow-covered saline ice. *IEEE Transactions on Geoscience and Remote Sensing 28*(4), 456-463.

Campbell, W. J. and 19 others (1978). Microwave remote sensing of sea ice in the AIDJEX main experiment. *Boundary layer meteorology 13*, 309-337.

Carlström, A. & L. M. H. Ulander (1993). C-band backscatter signatures of old sea ice in the Central Arctic during freeze-up. *IEEE Transactions on Geoscience and Remote Sensing 31*(4), 819-829.

Colbeck, S. C. (1989). Snow-crystal growth with varying surface temperatures and radiation penetration. *Journal of Glaciology 35*(119), 23-29.

Colbeck, S. C. (1990). The layered character of snow covers. *Reviews of Geophysics 29*(1), 81-96.

Comiso, J. T. C. Grenfell, D. L. Bell, M. A. Lange, & S. F. Ackley (1989). Passive microwave in situ observations of winter Weddell Sea ice. *Journal of Geophysical Research 94*(C8), 10891-10905.

CONVECTION (2001). Cruise report A/S Jan Mayen 2001, Convection. Fifth Framework Programme of the European Commission 1998-2002, Contract no. EVK2-2000-00058.

Dierking, W. (2001). Radar signatures of frazil and pancake ice – a review. CONVECTION Report No. 7. Fifth Framework Programme of the European Commission 1998-2002, Contract no. EVK2-2000-00058, p. 51.

Dierking, W. M. I. Petterson & J. Askne (1999). Multifrequency scatterometer measurements of Baltic sea ice during EMAC-95. *International Journal of Remote Sensing 20*(2), 349-372.

Dierking, W. Quantita tive roughness characterisation of geological surface and implications for radar signature analysis. *IEEE Transactions on Geoscience and Remote Sensing 37*(5), 2397-2412, 1999.

Dierking, W. Remote sensing course lecture notes. Technical University of Denmark, 2000.

Dierking, W., A. Carlström, L.M.H. Ulander. The effect of inhomogeneous roughness on radar backscattering from slightly deformed sea ice. *IEEE Transactions on Geoscience and Remote Sensing 35*(1), 147-159, 1997.

Drinkwater, M. R. (1989), LIMEX ’87 Ice surface characteristics: implications for C-band SAR backscatter signatures. *IEEE Transactions on Geoscience and Remote Sensing 27*(5), 501-513.

Fetterer, F. M., M. R. Drinkwater, K. C. Jezek, S. W. C. Laxon, R. G. Onstott, & L. M. H. Ulander (1992) Sea ice altimetry. In: F. D. Carsey (Ed.). *Microwave remote sensing of sea ice, Geophysical monograph 68* (pp. 111-135). Washington DC: American Geophysical Union.

Fofonoff, N. P. Physical properties of seawater: A new salinity scale and equation of state for seawater. Journal of Geophysical Research 90(C2), 3332-3342, 1985.

Fung, A. K. (1994). *Microwave Scattering and Emission Models and Their Applications*. Norwood MA: Artec House.

Garrity, C. (1992). Characterisation of snow on floating ice and case studies of brightness temperature changes during the onset of melt. In: F. D. Carsey (Ed.). *Microwave remote sensing of sea ice, Geophysical monograph 68* (pp. 313-328). Washington DC: American Geophysical Union.

Grenfell, T. C., D. J. Cavalieri, J. C. Comiso, M. R. Drinkwater, R. G. Onstott, I. Rubinstein, K. Steffen, & D. P. Winebrenner (1992). Considerations for microwave remote sensing of thin sea ice. In: F. D. Carsey (Ed.). *Microwave remote sensing of sea ice, Geophysical monograph 68* (pp. 291-301). Washington DC: American Geophysical Union.

Hallikainen, M., & D. P. Winnebrenner (1992). The physical basis for sea ice remote sensing. In: F. D. Carsey (Ed.). *Microwave remote sensing of sea ice, Geophysical monograph 68* (pp. 29-44). Washington DC: American Geophysical Union.

Hallikainen, M., F. T. Ulaby & M. Abdelrazik (1986). Dielectric properties of snow in the 3 to 37 GHz range. *IEEE Transactions on Antennas and Propagation 34*(11), 1329-1340.

Hoekstra, P. & P. Cappillino (1971). Dielectric properties of sea and sodium-cloride ice at UHF and microwave frequencies. *Journal of Geophysical Research 76*(20), 4922-4931.

Josberger, E. G. & N. M. Mognard (2002). A passive microwave snow depth algorithm with a proxy for snow metamorphism. *Hydrological Processes 16*, 1557-1568.

Martin, S., & P. Kauffman (1981). A field and laboratory study of wave damping by grease ice. *Journal of Glaciology 27*(96), 183-313.

Mätzler, C. (1987). Applications of the interaction of microwaves with the natural snow cover. *Remote Sensing Reviews 2*(2), 259-391.

Mätzler, C. Improved Born approximation for scattering of radiation in a granular medium. *Journal of Applied Physics 83*(11), 6111-6117, 1998.

Maykut, G. A. (1986). The surface heat and mass balance. In: N. Untersteiner (Ed.) *The Geophysics of Sea Ice*. NATO ASI series, series B: Physics Vol. 146 (pp. 395-463). New York & London: Plenum Press.

Nakawo, M., & N. K. Sinha (1981). Growth rate and salinity profile of first-year sea ice in the high Arctic. *Journal of Glaciology 27*, 315-330.

Nghiem, S. V., R. Kwok, S. H. Yueh, & M. R. Drinkwater (1995). Polarimetric signatures of sea ice – 2. Experimental observations. *Journal of Geophysical Research 100*(C7), 13681-13698.

Onstott, R. G. (1992). SAR and scatterometer signatures of sea ice. In: F. D. Carsey (Ed.). *Microwave remote sensing of sea ice, Geophysical monograph 68* (pp. 73-104). Washington DC: American Geophysical Union.

Onstott, R. G., P. Gogineni, A. J. Gow, T. C. Grenfell, K. C. Jezek, D. K. Perovich, & C. T. Swift (1998). Electromagnetic and physical properties of sea ice in the presence of wave action. *IEEE Transactions on Geoscience and Remote Sensing 36*(5), 1764-1783.

Polder, D. & J. H. Van Santen (1946). The Effective permeability of mixtures of solids, *Physica XII*(5), 257-271.

Rothrock, D. A., Ice thickness distribution – measurement and theory. In: N. Untersteiner (Ed.). *The Geophysics of Sea Ice* (pp. 551-575). NATO ASI series, Series B: Physics Vol. 146. Plenum Press, 1986.

Shen, H. H., S. F. Ackley, & M. A. Hopkins (2001). A conceptual model for pancake-ice formation in a wave field. *Annals of Glaciology 33*, 361-367.

Shokr, M. E. (1998). Field Observations and model calculations of dielectric properties of Arctic sea ice in the microwave C-band. *IEEE Transactions on Geoscience and Remote Sensing 36*(2), 463-478.

Tucker, W. B., D. K. Perowich, A. J. Gow, W. F. Weeks, & M. R. Drinkwater (1992). Physical properties of sea ice relevant to remote sensing. In: F. D. Carsey (Ed.). *Microwave remote sensing of sea ice, Geophysical monograph 68* (pp. 9-28). Washington DC: American Geophysical Union.

Tucker, W. B., T. C. Grenfell, R. G. Onstott, D. K. Perovich, A. J. Gow, R. A. Shuchman & L. Sutherland (1991). Microwave and physical properties of sea ice in the winter marginal ice zone. *Journal of Geophysical Research 96*(C3), 4573-4587.

Ulaby, F. T., R. K. Moore & A. K. Fung (1981). *Microwave Remote Sensing, Fundamentals and Radiometry, vol. 1*. Dedham MA: Artech House.

Ulaby, F. T., R. K. Moore & A. K. Fung (1986). *Microwave Remote Sensing, From Theory to Applications, vol. 3*. Dedham MA: Artech House.

Ulander, L. M. H., A. Carlström & J. Askne (1995). Effects of frost flowers, rough saline snow and slush

on the ERS-1 SAR backscatter of thin Arctic sea-ice. *International Journal of Remote Sensing 16*(17), 3287-3305.

Vant, M. R., R. B. Gray, R. O. Ramseier, & V. Makios (1974). Dielectric properties of fresh and sea ice at 10 and 35 GHz. *Journal of Applied Physics 45*(11), 4712-4717.

Vant, M. R., R. O. Ramseier & V. Makios (1978). The complex-dielectric constant of sea ice at frequencies in the range 0.1-40GHz. *Journal of Applied Physics 49*(3), 1264-1280.

Wadhams, P. (2000). *Ice in the Ocean.* Gordon & Breach Science Publishers.

Wadhams, P., J. C. Comiso, E. Prussen, S. Wells, M. Brandon, E. Aldworth, T. Viehoff, R. Allegrino & D. R. Crane (1996). The development of the Odden ice tongue in the Greenland Sea during winter 1993 from remote sensing and field observations. *Journal of Geophysical Research 101*(C8), 18213-18235.

Warren, S. G., I. G. Rigor, N. Untersteiner, V. F. Radionov, N. N. Bryazgin, Y. I. Aleksandrov, R. Colony. Snow depth on Arctic sea ice. *Journal of Climate 12*, 1814-1829, 1999.

Weeks, W. F., & S. F. Ackley (1986). The growth, structure, and properties of sea ice. In N. Untersteiner (Ed.), *The geophysics of sea ice*. (pp. 9-164). New York: Plenum Press.

Winebrenner, D. P., J. Bredow, A. K. Fung, M. R. Drinkwater, S. Nghiem, A. J. Gow, D. K. Perowich, T. C. Grenfell, H. C. Han, J. A. Kong, J. K. Lee, S. Mudaliar, R. G. Onstott, L. Tsang, R. D. West (1992). Microwave sea ice signature modelling. In: F. D. Carsey (Ed.). *Microwave remote sensing of sea ice, Geophysical monograph 68* (pp. 137-175). Washington DC: American Geophysical Union.

Previous reports

Previous reports from the Danish Meteorological Institute can be found on: http://www.dmi.dk/dmi/dmi-publikationer.htm